RSC Advances

ROYAL SOCIETY OF CHEMISTRY

www.rsc.org/advances

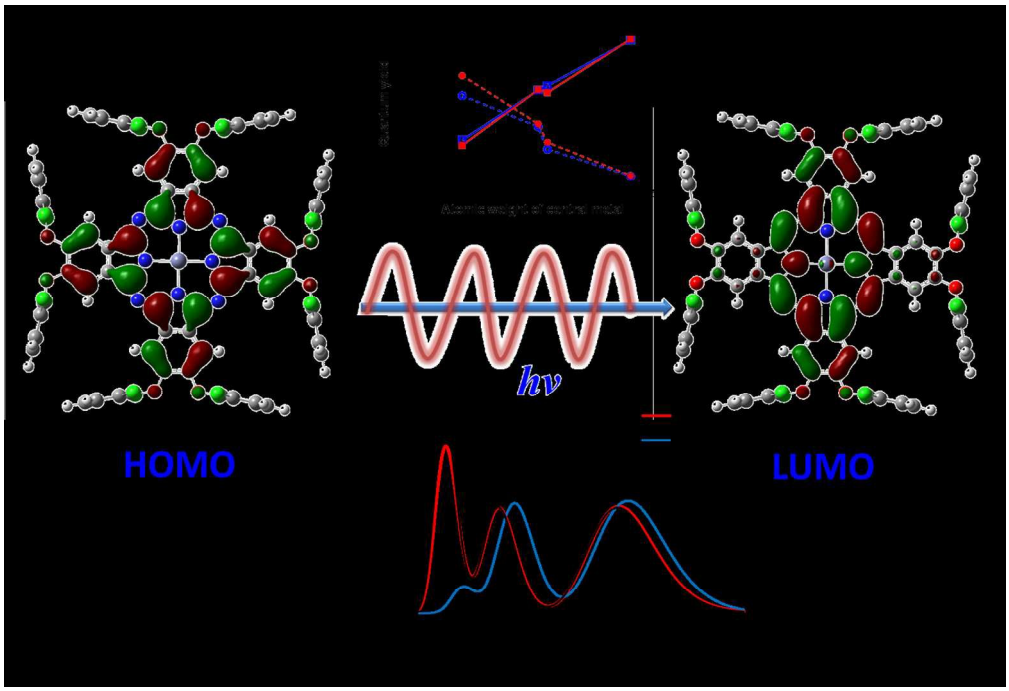

DFT and TD-DFT computational studies validated the experimental results and revealing details about the electronic structures of novel halogenated phthalocyanines. Fluorescence and singlet oxygen quantum yields analysis revealed two-dimensional heavy atom effect that influenced the photophysical parameters.
249x169mm (150 x 150 DPI)

Journal Name

RSCPublishing

Cite this: DOI: 10.1039/x0xx00000x

Photophysical and theoretical studies of peripherally halogenated octaphenoxyphthalocyanines

Saad Makhseed,[a,*] Basma Ghazal,[a] Amr Mohamed Abdelmoniem,[a] Veronika Novakova,[b] and Petr Zimcik[c],

Received 00th January 2012,
Accepted 00th January 2012

DOI: 10.1039/x0xx00000x

www.rsc.org/

Peripherally substituted phthalocyanines with halogenated phenoxy groups containing different central metals (In(III), Ga(III), Mg(II) and Zn(II)) were synthesized. The X-ray analyses confirmed that the halogen atoms (Cl, Br) at the *ortho* positions were bulky enough to orient the phenoxy substituents perpendicularly relative to the Pc core and perfectly discouraged cofacial aggregation. The ground state geometry, HOMO/LUMO energies and the electronic properties were theoretically calculated for some complexes and corresponded well with experimental data. Analysis of fluorescence and singlet oxygen quantum yields revealed strong heavy atom effect provided by the central metal. Irrespective of the present halogen, indium(III) complexes were characterized by high singlet oxygen production and very low fluorescence while reverse data were obtained for Mg(II) complexes.

Introduction

Phthalocyanines (Pcs), a versatile class of organic functional materials, are widely used in large variety of applications due to their outstanding optical and electronic properties combined with excellent thermal and chemical stability.[1-5] However, controlling the Pc bulk material on a molecular level is a crucial requirement to improve the desired photophysical and opto(electronic) properties which can maximize their potential utility in the intended applications.[6-10] Therefore, the Pc self-association represents the main limitation barrier of using such material in optical related application such as photodynamic therapy (PDT) or optical limiting.[11-17] Many strategies have been attempted by several groups over the last decades to overcome the detrimental influence of aggregation by yielding new Pc materials with unique photophysical and optoelectronic properties tailored to the required applications.[18-21] Recently, we found that the bulky substituents of 2,3,9,10,16,17,23,24-octakis(2,6-di-*iso*-propylphenoxy) phthalocyaninato zinc(II) (**Pc1-Zn**) effectively prohibited self-association of the macrocycle even within solid thin films[22] and resulted in the formation of unique nanoporous cubic crystals.[23] Introduction of different metals such as zinc, indium and gallium into the central Pc rings could lead to the formation of Pc derivatives with high triplet quantum yield[24] which can be considered as a crucial requirement for efficient photosensitizers in PDT application. Similarly, also peripheral substituents may substantially influence photophysical properties. It should be also noted that the halogenated phthalocyanines showed promising photoelectric properties due to the heavy atom effect (i.e. spin-orbit coupling effect).[25] Moreover, presence of halogen atoms lowers both the fluorescence quantum yield and the fluorescence lifetime, enhances the triplet quantum yield and decreases the triplet lifetime.[26]

Considerable efforts have been made to explain the electronic structures of MPcs using theoretical calculations. The density functional theory (DFT) calculations were used to investigate the geometric structures and the electronic properties of several MPc complexes. TD-DFT calculations were also used to study the electronic behavior aspects of the Pcs, including the molecular geometries, ground-state and excited-state electronic structures, vibrational spectra and absorption spectra.[27-34]

Inspired by aforementioned findings, we proposed the synthesis of new Pc derivatives peripherally substituted with phenoxy groups decorated by halogen atoms with different metal ions (Ga, In, Mg, Zn) coordinated in the newly prepared Pc complexes to investigate their impact on photophysical features. In addition theoretical investigation of halogenated phthalocyanines were conducted on selected complexes (**Pc2-Zn** and **Pc3-Zn**) to evaluate their electronic properties. The molecular structures of the studied complexes were optimized using the B3LYP/SDD method and compared with a previously reported non-halogenated complex (**Pc1-Zn**).[25]

Experimental

General Procedures

Among the starting materials, 2,6-dichlorophenol and 2,6-dibromophenol were purchased from Sigma-Aldrich and used directly without further purification. 4,5-Dichlorophthalonitrile (**Pn1**) was synthesized according to the literature method.[35] Anhydrous cesium fluoride and unsubstituted zinc phthalocyanine were purchased from Sigma-Aldrich and used as received. TLC was performed using Polygram sil G/UV 254 TLC plates and visualization was carried out by ultraviolet light

at 254 nm and 350 nm. Column chromatography was performed using Merck silica gel 60 of mesh size 0.040–0.063 mm. Anhydrous solvents were either supplied from Sigma-Aldrich and used as they were received or dried as described by Perrin.[36] ^{1}H and ^{13}C NMR Spectra were recorded using Bruker DPX 400 at 400 MHz and 100 MHz respectively and IR spectra were obtained from Jasco 6300 FTIR. UV–Vis studies were done on a Varian Cary 5 spectrometer and Shimadzu UV-2600 spectrophotometer. Elemental analyses were carried out using ElementarVario Micro Cube. High resolution mass analyses (HRMS) were measured on Xevo G2-S QTof (Waters). In addition, clusters of peaks that correspond to the calculated isotope composition of the molecular ion were observed by matrix-assisted laser desorption ionization mass spectroscopy (MALDI-TOF) *via* ultrafleXtreme (Bruker). The MALDI-TOF mass data for Pcs are presented as the mass of the most intense peak in the cluster instead of exact mass. The calculated exact mass is beyond the detection of the instrument as its abundance is very low (e.g. for brominated Pcs below 0.01 %). Melting points were determined *via* differential scanning calorimetry (DSC) analyses on Shimadzu DSC-50. Single crystal data collections were made on a Rigaku R-Axis Rapid diffractometer using filtered Mo-Kα radiation. The diffraction data were collected at a temperature of -123 °C (Oxford cryosystems). The fluorescence spectra were obtained using an AMINCO Bowman Series 2 luminescence spectrometer and are uncorrected.

General method for synthesis of phthalonitriles Pn2 and Pn3. To a stirred solution of 2,6-dihalophenol (2.5 equiv) and 4,5-dichlorophthalonitrile (1 equiv) in dry DMF (10 ml) under nitrogen atmosphere, anhydrous cesium fluoride (5 equiv) was added. The reaction mixture was further heated at 110 °C for 48 h. The reaction mixture, after being cooled, was poured into distilled water and the resulting precipitate was collected by filtration and washed several times with distilled water, then air-dried. Afterwards, the crude product was purified by column chromatography on silica eluting with dichloromethane:hexane (1:2, v/v) mixture to receive the desired product.

4,5-Bis(2,6-dichlorophenoxy)phthalonitrile (Pn2). The disubstituted phthalonitrile **Pn2** was prepared from 2,6-dichlorophenol (4.08 g, 25 mmol) using the above mentioned general procedure and was received as a white powder (Yield: 3.46 g, 77 %); M.p: 245 °C; IR (KBr) ν/cm^{-1} 3424, 2232 (CN), 1597, 1504, 1444; ^{1}H NMR (DMSO-d$_6$, 400 MHz) δ/ppm = 7.44 (s, 2H, ArH), 7.63 (t, 2H, ArH), 7.77 (d, 4H, ArH); ^{13}C NMR ($CDCl_3$, 100 MHz) δ/ppm =110.64, 114.98, 119.84, 127.92, 128.75, 130.09, 144.53, 148.19. HRMS (ESI) calc. for $C_{20}H_8Cl_4N_2O_2$ $[M]^+$: 447.9340, found 447.9351 $[M]^+$; elemental analysis calcd (%) for $C_{20}H_8Cl_4N_2O_2$: C, 53.37; H, 1.79; N, 6.22 found: C, 53.23; H, 1.56; N, 6.15.

4,5-Bis(2,6-dibromophenoxy)phthalonitrile (Pn3). The disubstituted phthalonitrile **Pn3** was prepared from 2,6-dibromophenol (6.30 g, 25 mmol) using the above mentioned general procedure and was received as a white solid (yield: 4.4 g, 70 %); M.p = 281 °C; IR (KBr) ν/cm^{-1}= 3424, 2229 (CN) 1596, 1563; ^{1}H NMR ($CDCl_3$, 400 MHz) δ/ppm = 6.82 (s, 2H, ArH), 7.20 (t, 2H, ArH), 7.72 (d, 4H, ArH); ^{13}C NMR ($CDCl_3$, 100 MHz) δ/ppm = 110.63, 114.94, 117.83, 118.74, 129.16, 133.54, 147.13, 148.49. HRMS (ESI) calc. for $C_{20}H_8Br_4N_2O_2$ $[M]^+$: 623.7319, found 623.7291 $[M]^+$; elemental analysis calcd (%) for $C_{20}H_8Br_4N_2O_2$: C, 38.26; H, 1.28; N, 4.46 found: 38.61; H, 1.35; N, 4.64.

General methods for the synthesis of metallophthalocyanines (Pc2-M, Pc3-M). *Method A*: To a stirred solution of **Pn2** or **Pn3** (0.5 g) in dry quinoline (3 mL), an excess amount of anhydrous metal salt (4 molar equiv.) was added and the mixture was heated at 180 °C for 12 h under nitrogen. On cooling, the reaction mixture was poured into distilled water. The resulting green solid was collected and purified by column chromatography on silica using the appropriate eluent as stated for each complex below. Furthermore, the product was re-precipitated by dissolving in chloroform and dropping into hot methanol to receive the pure complex as a dark green powder.

Method B: An excess amount of anhydrous metal salt (4 molar equiv.) and a catalytic amount of 1,8-diazabicyclo[5.4.0]undec-7-ene (DBU, 2-3 drops) were mixed with **Pn2** or **Pn3** (0.5 g) in dry pentanol (3 mL) and the reaction mixture was stirred at 140 °C for 24 h under nitrogen. The reaction mixture was then poured into 50 % aqueous methanol. The crude product was collected by filtration and purified by the same way described in method A to receive pure green products.

2,3,9,10,16,17,23,24-Octakis(2,6-dichlorophenoxy) phthalocyaninato zinc(II) (Pc2-Zn). Anhydrous $Zn(OAc)_2$ as metal salt. The solvent system used for the column purification was $CHCl_3$: EtOAc (1:1, v/v) (yield: 93 mg, 18 % (method A); 103 mg, 20 % (method B)). M.p. over 300 °C; UV-vis (THF) λ/nm (ε/M^{-1} cm^{-1}): 671 (334720), 642 (44032), 606 (49517), 359 (116350); IR (KBr) ν/cm^{-1} = 3065, 2916, 2850, 1609, 1570, 1545, 1489, 1477, 1443, 1400, 1340, 1275, 1240, 1205, 1171, 1136, 1092, 1067, 1024, 893, 866, 812, 791, 768, 746, 714; ^{1}H NMR (400 MHz; DMSO-d$_6$) δ/ppm = 7.83 (t, 8H, ArH), 7.88 (d, 16H, ArH), 8.00 (s, 8H, ArH); Anal. calc. for $C_{80}H_{32}Cl_{16}N_8O_8Zn$ + $2H_2O$: C, 50.52; H, 1.91; N, 5.89, found C, 50.67; H, 2.17; N, 5.97; MS (MALDI-TOF) (m/z): 1866 $[M]^+$.

2,3,9,10,16,17,23,24-Octakis(2,6-dichlorophenoxy) phthalocyaninato magnesium(II) (Pc2-Mg). $Mg(OAc)_2.4H_2O$ as the metal salt. The solvent system used for the column purification was CH_2Cl_2: hexane (2:1, v/v) followed by $CHCl_3$ (yield: 76 mg, 15 % (method A); 96 mg, 19 % (method B)). M.p. over 300 °C; UV-vis (THF) λ/nm (ε/M^{-1} cm^{-1}): 672 (295620), 643 (40805), 609 (43124), 362 (115620); IR (KBr) ν/cm^{-1} = 3067, 2993, 2924, 2829, 1657, 1639, 1610, 1569, 1545, 1526, 1483, 1443, 1396, 1340, 1277, 1242, 1207, 1169, 1134, 1084, 1022, 895, 866, 791, 771, 752, 715, 536; ^{1}H NMR (400 MHz; $CDCl_3$:DMSO-d$_6$ (5:1)) δ/ppm = 7.60 (t, 8H, ArH), 7.72 (d, 16H, ArH), 8.1 (s, 8H, ArH); Anal. calc. for $C_{80}H_{32}Cl_{16}MgN_8O_8$: C, 52.66; H, 1.77; N, 6.14, found C 52.63, H 2.38, N 6.29; MS (MALDI- TOF)(m/z): 1823 $[M]^+$.

2,3,9,10,16,17,23,24-Octakis(2,6-dichlorophenoxy) phthalocyaninato gallium(III) chloride (Pc2-Ga). Anhydrous $GaCl_3$ as the metal salt. The solvent system used for the column purification was CH_2Cl_2:hexane (2:1, v/v) followed by $CHCl_3$:DMF

(50:1, v/v) (yield: 31 mg, 15 % (method A); 29 mg, 14 % (method B)). M.p. over 300 °C; UV-vis (THF) λ/nm (ε/M^{-1} cm^{-1}): 683 (248660), 652 (35933), 616 (38544), 366 (97640); IR (KBr)ν/cm^{-1} = 3069, 2923, 2851, 1608, 1572, 1487, 1443, 1400, 1342, 1277, 1242, 1205, 1175, 1134, 1092, 1026, 899, 874, 793, 770, 744, 712; ^{1}H NMR (400 MHz; DMSO-d_6) δ/ppm = 7.93 (t, 8H, ArH), 8.02 (d, 16H, ArH), 8.14 (s, 8H, ArH); Anal. calc. for $C_{80}H_{32}Cl_{17}GaN_8O_8$: C, 50.43; H, 1.69; N, 5.88, found C, 50.28; H, 1.52; N, 5.69; MS (MALDI-TOF)(m/z): 1905 [M^+].

2,3,9,10,16,17,23,24-Octakis(2,6-dichlorophenoxy) phthalocyaninato indium(III) chloride (Pc2-In). Anhydrous $InCl_3$ as the metal salt. The solvent system used for the column purification was CH_2Cl_2:hexane (2:1, v/v) followed by EtOAc:DMF (1:1, v/v) (yield: 88 mg, 17 % (method A); 103 mg, 20 % (method B)). M.p. over 300 °C; UV-vis (THF) λ/nm (ε/M^{-1} cm^{-1}): 691 (239400), 658 (38033), 623 (40300), 368 (100520); IR (KBr) ν/cm^{-1} = 3067, 1724, 1671, 1611, 1571, 1486, 1442, 1399, 1340, 1278, 1240, 1205, 1173, 1135, 1091, 1025, 898, 865, 793, 769, 742, 714, 535; ^{1}H NMR (400 MHz; $CDCl_3$) δ/ppm = 7.36 (t, 8H, ArH), 7.83 (d, 16H, ArH), 8.13 (s, 8H, ArH); Anal. calc. for $C_{80}H_{32}Cl_{17}InN_8O_8$: C, 49.26; H, 1.65; N, 5.74, found C, 49.48; H, 1.78; N, 5.52; MS (MALDI-TOF)(m/z): 1949 [$M]^+$.

2,3,9,10,16,17,23,24-Octakis(2,6-dibromophenoxy) phthalocyaninato zinc(II) (Pc3-Zn). Anhydrous $Zn(OAc)_2$ as the metal salt. The solvent system used for the column purification was $CHCl_3$:EtOAc (2:1, v/v) (yield: 92 mg, 18 % (method A); 107 mg, 21 % (method B)). M.p. over 300 °C; UV-vis (THF) λ/nm (ε/M^{-1} cm^{-1}): 673 (327260), 642 (44031), 609 (45518), 358 (112200); IR (KBr) ν/cm^{-1} = 3418, 3064, 2953, 1721, 1611, 1576, 1561, 1486, 1470, 1456, 1433, 1399, 1340, 1273, 1230, 1170, 1136, 1092, 1045, 1027, 947, 894, 864, 808, 768, 746, 725, 658; ^{1}H NMR (400 MHz; $CDCl_3$:DMSO-d_6 (5:1)) δ/ppm = 7.42 (t, 8H, ArH), 7.87 (d, 16H, ArH), 8.10 (s, 1H, ArH); Anal. calc. for $C_{80}H_{32}Br_{16}N_8O_8Zn$: 37.29; H, 1.25; N, 4.35, found C 37.58, H 1.19, N 4.76; MS (MALDI-TOF)(m/z): 2577 [M^+].

2,3,9,10,16,17,23,24-Octakis(2,6-dibromophenoxy) phthalocyaninato magnesium(II) (Pc3-Mg). $Mg(OAc)_2.4H_2O$ as the metal salt. The solvent system used for the column purification was $CHCl_3$:hexane (2:1, v/v) followed by $CHCl_3$:EtOAc (1:1, v/v) (yield: 80 mg, 16 % (method A); 95 mg, 19 % (method B)). M.p. over 300 °C; UV-vis (THF) λ/nm (ε/M^{-1} cm^{-1}): 675 (276210), 642 (40468), 610 (43366), 363 (123360); IR (KBr) ν/cm^{-1} = 3065, 2868, 2833, 1611, 1560, 1470, 1455, 1433, 1396, 1339, 1273, 1233, 1168, 1133, 1085, 1046, 1025, 946, 894, 864, 807, 768, 752, 724, 521; ^{1}H NMR (400 MHz; $CDCl_3$:DMSO-d_6 (5:1)) δ/ppm = 7.29 (t, 8H, ArH), 7.79 (d, 16H, ArH), 8.15 (s, 8H, ArH); Anal. calc. for $C_{80}H_{32}Br_{16}MgN_8O_8$: C, 37.89; H, 1.27; N, 4.42, found C, 37.55; H, 1.09; N, 4.61; MS (MALDI-TOF)(m/z): 2535 [$M]^+$.

2,3,9,10,16,17,23,24-Octakis(2,6-dibromophenoxy) phthalocyaninato gallium(III) chloride (Pc3-Ga). Anhydrous $GaCl_3$ as the metal salt. The solvent system used for the column purification was $CHCl_3$:EtOAc (2:1, v/v) followed by $CHCl_3$:DMF (50:1, v/v) (yield: 78 mg, 15 % (method A); 62 mg, 12 % (method B)). M.p over 300 °C; UV-vis (THF) λ/nm (ε/M^{-1} cm^{-1}): 684 (296330), 649 (37295), 619 (45577), 368 (118200); IR (KBr) ν/cm^{-1}= 3067, 2961, 1666, 1611, 1561, 1506, 1458, 1432, 1405, 1343, 1278, 1237, 1173, 1145, 1095, 1072, 1034, 1001, 898, 804, 768, 748, 725, 545, 521; ^{1}H NMR (400 MHz; $CDCl_3$) δ/ppm = 7.39 (t, 8H, ArH), 7.88 (d, 16H, ArH), 8.18 (s, 1H, ArH); Anal. calc. for $C_{80}H_{32}Br_{16}ClGaN_8O_8$: C, 36.72; H, 1.23; N, 4.28, found C, 36.58; H, 1.09; N, 4.16; MS (MALDI-TOF)(m/z): 2616 [$M]^+$.

2,3,9,10,16,17,23,24-Octakis(2,6-dibromophenoxy) phthalocyaninato indium(III) chloride (Pc3-In). Anhydrous $InCl_3$ as the metal salt. The solvent system used for the column purification was $CHCl_3$:EtOAc (2:1, v/v) (yield: 84 mg, 16 % (method A); 79 mg, 15 % (method B)). M.p. over 300 °C; UV-vis (THF) λ/nm (ε/M^{-1} cm^{-1}): 693 (300590), 664 (47080), 625 (50661), 369 (120750); IR (KBr) ν/cm^{-1} = 3066, 1724, 1663, 1607, 1560, 1485, 1454, 1431, 1393, 1335, 1276, 1242, 1170, 1135, 1093, 1068, 1044, 1026, 993, 896, 875, 799, 767, 742, 725, 520; ^{1}H NMR (400 MHz; $CDCl_3$) δ/ppm = 7.36 (t, 8H, ArH), 7.83 (d, 16H, ArH), 8.13 (s, 8H, ArH); Anal. calc. for $C_{80}H_{32}Br_{16}ClInN_8O_8$: C, 36.10; H, 1.21; N, 4.21, found C 36.25, H 1.09, N 3,98; MS (MALDI-TOF)(m/z): 2661 [$M]^+$.

Computational details

DFT have been implemented to obtain the most energetically stable geometry and molecular orbitals. TD-DFT were further carried out on the optimized geometry to generate the electronic absorption spectra of some halogenated phthalocyanine complexes (**Pc2-Zn** and **Pc3-Zn**) compared with the previously reported non-halogenated **Pc1-Zn**. The aforementioned methods were successfully used to calculate the energy minimized structure, molecular orbitals and electronic absorption spectra of the target complexes.[30-33] Geometry optimization and frequency calculations of this symmetrical Pc derivatives were calculated at the density functional B3LYP level with the SDD basis set.[37,38] Forty states of each compound were considered in the TD-DFT calculations. All of the calculations were performed using Gaussian09W Multiprocessor/core version (64-bit) RevD software package.[39] The final optimized structures were visualized using Gaussview version 5.0.9 and Chemcraft software packages. [40,41]

Fluorescence quantum yields

All samples were repurified before photophysical measurements by preparative TLC (Merck Kieselgel 60 F_{254}) to ensure high purity of the samples using the following eluents: toluene:THF 10:1 (for **Pc2-Zn**, **Pc2-Mg**, **Pc3-Zn** and **Pc3-Mg**), MeOH followed by chloroform:THF 10:1 (for **Pc2-In** and **Pc3-In**) or MeOH followed by chloroform:THF 20:1 (for **Pc2-Ga** and **Pc3-Ga**). The corresponding green spots were scraped and the pure product was extracted from silica using chloroform:pyridine 1:1 (for **Pc2-In** and **Pc3-In**) or THF (the rest of the samples), filtered and evaporated to dryness. Fluorescence quantum yields (Φ_F) of the studied Pcs were determined by comparative method in THF and calculated using the following equation (Eq. (1)):

$$\Phi_F^S = \Phi_F^R \left(\frac{F^S}{F^R}\right)\left(\frac{1-10^{-A^R}}{1-10^{-A^S}}\right) \quad \text{(Eq. 1)}$$

where the terms, Φ_F, F and A denote the fluorescence quantum yield, the area under the fluorescence emission curve and the absorbance at the excitation wavelength, respectively. The superscripts R and S point to reference and sample, respectively. Unsubstituted zinc phthalocyanine (ZnPc) was employed as the reference ($\Phi_{F(THF)}$ = 0.32).[12] Both reference and sample were excited at the same wavelength (λ_{exc} = 610 nm). The absorbance at Q-band maximum was adjusted to be lower than 0.05 aiming to eliminate the inner filter effect. The recorded data in all the experiments are the mean of three independent measurements with an estimated error of ±10 %. Excitation spectra were collected by observing fluorescence signal usually at 720 nm.

Singlet oxygen quantum yields

The quantum yields of the singlet oxygen (Φ_Δ) were determined in THF according to a slightly modified published procedure[42] using the decomposition of a chemical trap 1,3-diphenylisobenzofuran (DPBF) with ZnPc as a reference (Φ_Δ= 0.53 in THF).[43] The detailed procedure was as follows: 2.5 mL of a DPBF stock solution in THF (5×10^{-5} M) was transferred into a 10 × 10 mm quartz optical cell and was saturated with oxygen for 1 min. A stock solution of the tested compound in THF (typically 30 µL) was then added to achieve an absorbance of the final solution in the Q-band maximum of approximately 0.1. The solution was stirred and irradiated using a xenon lamp (100 W, ozone-free XE DC short-arc lamp, Newport). The incident light was filtered through a water filter (6 cm) and an OG530 cut-off filter (Newport) to remove the heat and the light below 523 nm, respectively. Decrease of DPBF in solution with irradiation time was monitored at 414 nm. All experiments were performed in triplicate, and the data presented herein represent the mean of the three experiments (estimated error: ± 10%).

Results and Discussions

Synthesis

The synthetic procedure for preparing the target halogenated phthalocyanine derivatives (**Pc2-M**, **Pc3-M**) is depicted in Scheme 1. The starting phthalonitrile precursors **Pn2** and **Pn3** were prepared in a good yield (~ 70%) from the conventional aromatic nucleophilic substitution reaction between 4,5-dichlorophthalonitrile (**Pn1**) with the 2,6-dihalogenated phenols (2,6-dichlorophenol and 2,6-dibromophenol) using DMF as solvent in the presence of anhydrous CsF. Unfortunately, the fluorinated and iodinated phenols failed to produce the corresponding phthalonitriles and gave cross-linked material and mono-substituted phthalonitrile in very low yield, respectively. Subsequently, the prepared phthalonitriles **Pn2** and **Pn3** underwent metal-mediated cyclotetramerization in quinoline or pentanol/DBU using the appropriate metal salt: $Zn(OAc)_2$, $Mg(OAc)_2$, $GaCl_3$ and $InCl_3$ to afford the corresponding phthalocyanine derivatives **Pc2-M** and **Pc3-M** in reasonable yields. The solubility of the prepared complexes was found to be excellent in most organic solvents (e.g. DCM, chloroform, toluene, ethyl acetate and THF) which facilitated their purification using column chromatography. Structural identifications and purity of the prepared complexes were confirmed by various characterization techniques such as ^{1}H NMR, UV/Vis, IR and elemental analysis which gave results consistent with the proposed complex structures.

The complexes were further characterized by MALDI-TOF spectrometry that confirmed the mass corresponding to the expected values. Some of them showed the proposed calculated masses only Fig. S10, others gave spectra with fragments corresponding to loss of some halogen atoms. For example, the spectrum of **Pc3-Zn** consists of a cluster of molecular ion peaks centered at 2577 which is assigned to the corresponding mass of Pc complex. However, other clusters also appeared in the spectrum as a consequence of fragmentation. Their *m/z* matched the complex missing one and more bromine atoms as depicted in Fig. 1 The experimental isotopic pattern perfectly agreed with the theoretical one.

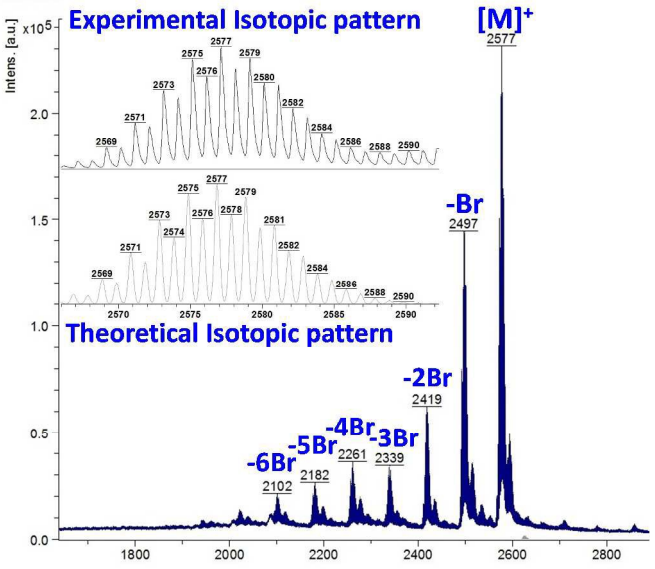

Fig. 1 MALDI-TOF (m/z) spectra and isotopic distribution of **Pc3-Zn.**

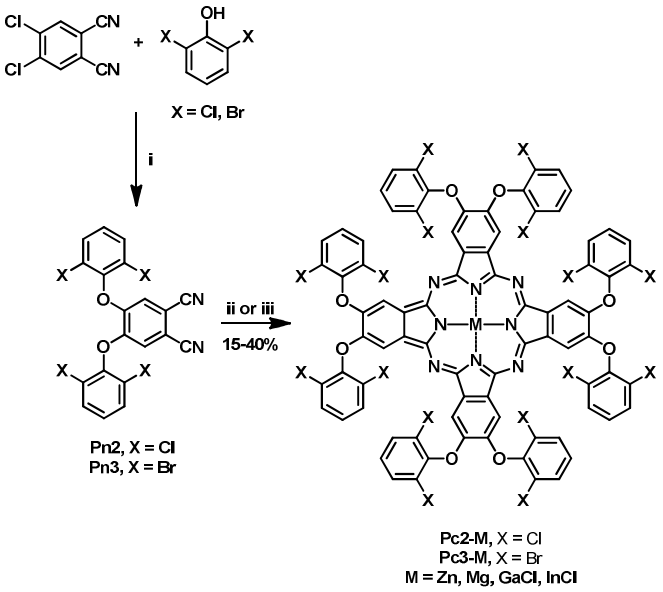

Scheme 1. Synthesis of complexes **Pc2-M** and **Pc3-M**. *Reagents and conditions*: (i) DMF, anhydrous CsF, 110 °C, 48 h; (ii) appropriate metal salt, quinoline, 180 °C, 12 h; (iii) *n*-pentanol, DBU, appropriate metal salt, 140 °C, 24 h.

Structural and self-association characterization

The intrinsic behavior of disc-like phthalocyanine molecules arising from the π-π stacking can negatively affect their opto-electronic properties and greatly limit their efficiency in many intended applications. Therefore, many structural modification protocols have been adapted to control the degree of molecular self-association. UV-Vis and NMR spectroscopic techniques are the best tools to evaluate the aggregation behavior of phthalocyanine molecules. Aggregated Pcs can be detected by ^{1}H NMR spectrum exhibiting characteristic broad peaks. UV-Vis spectra can also be used to assess the aggregation from the position and the shape of the corresponding Q-band.

The ^{1}H NMR spectra of the prepared complexes **Pc2-M** and **Pc3-M** were recorded in either DMSO or $CDCl_3$ and exhibited well resolved spectra. In addition to this, the spectra of these complexes exhibited the same high quality as their corresponding precursors (**Pn2** and **Pn3**) and the previously reported non-aggregating **Pc1-Zn**.[25] As shown in Fig. 2, the NMR spectra of **Pc2-Zn** and its precursor **Pn2** show three distinct sharp signals in the aromatic region (triplet, doublet and singlet). The good quality of the obtained spectra was found to be unaffected by the concentration and remained unchanged with well resolved signals even at high concentration (2×10^{-2} M). Such behavior can be clearly attributed to the steric hindrance exerted by the peripheral phenoxy substituents bearing halogen atoms that lie almost perpendicular to the plane of the Pc core and consequently prevent the efficient π–π stacking of the macrocycle units. This conformation adapted by the bulky phenoxy groups was evidently confirmed by the X-ray analyses as shown in the Supporting information and discussed below.

The complex **Pc2-Zn** was examined using the NMR technique at variable temperatures (25-95 °C) (Fig. S11). The three signals in the **Pc2-Zn** spectrum moved apart from each other at higher temperature. However, the good quality of the spectrum remained unchanged. The doublet and triplet which belong to the phenoxy substituents shifted slightly into up field region whereas the singlet which belongs to the Pc core shifted into the down field area. This can be attributed to the increased free rotation around aryl ether linkage at high temperature which can decrease the ring current effect of the Pc ring. Conversely, such rotations move the Pc core proton within the proximity effect of the halogen atoms, therefore, the downfield shift of the singlet signal was recognized at high temperature due to the current effects exerted by the halogen atom.

Further assessment of the aggregation behavior of the prepared complexes was performed using UV-Vis spectroscopy technique. As anticipated, the sharp unperturbed single Q-band, typical of monomeric species, was the characteristic feature of all the complexes spectra in different organic solvents (DCM, $CHCl_3$, THF and DMF). For example, the absorption spectrum of **Pc2-Zn** showed a single sharp Q-band at λ_{max} = 671 nm (Fig. 3 and Table 1) which is typical for non-aggregated species belonging to D_{4h} symmetry. Further aggregation evaluation was performed by tracing the Q-band appearance and its position at different concentrations ranging from 10×10^{-6} M to 100×10^{-6} M. There were no spectral changes as the concentration varied within the studied concentration range, confirming that these complexes remained in truly monomeric form. As depicted in (Fig. 3), the Q-band absorption maximum of **Pc2-Zn** at 671 nm, perfectly follows the Lambert-Beer law in the studied concentration range and its molar extinction coefficient remained constant indicating a purely monomeric form. Another confirmation of non-aggregated character of the spectra is a perfect accordance of excitation spectra with the absorption spectra (see below). According to the aforementioned results based on the NMR and UV-visible spectroscopic analysis, the non-aggregating nature of the prepared Pc systems is well established even at higher solution concentrations. This achievement emphasized that the steric factor of halogen atoms in *ortho* position (e.g. chlorine and bromine) is sufficiently enough to keep the orthogonal conformation of phenoxy substituents relative to the Pc core.

For comparison, octasubstituted zinc Pcs with phenoxy groups bearing a variety of electron-withdrawing and -donating groups at the *para* position were found to be in aggregated form at concentration over 1×10^{-5} M in DMSO or $CHCl_3$ even bearing bulky *t*Bu substituent.[44] Substituents placed in *meta* positions on aryloxy substituents typically inhibit the aggregation well[45,46] but examples of aggregated derivatives may be found[47,48] in literature. Indeed, the tendency to aggregations decreases in order of *para* > *meta* > *ortho* substitution[49] of the peripheral aryloxy substituent as suggested also by a study of mesomorphic properties of different Pcs. For this reason, substitution of phenoxy substituents in *ortho* positions seems to be crucial for efficient inhibition of aggregation.

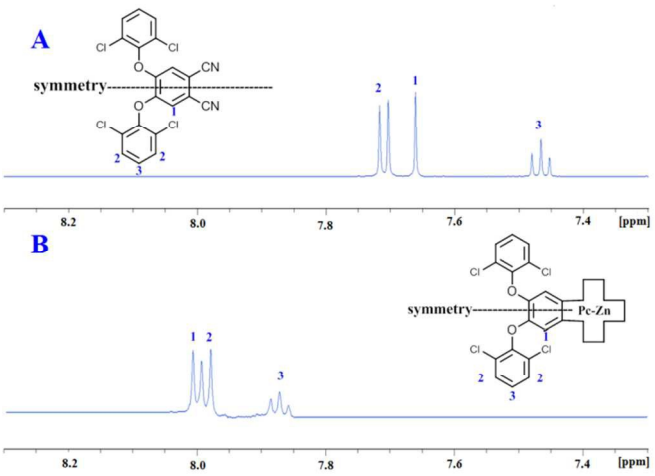

Fig. 2 A: ^{1}H NMR of phthalonitrile **Pn2** in DMSO-d_6; B: ^{1}H NMR of **Pc2-Zn** in DMSO-d_6.

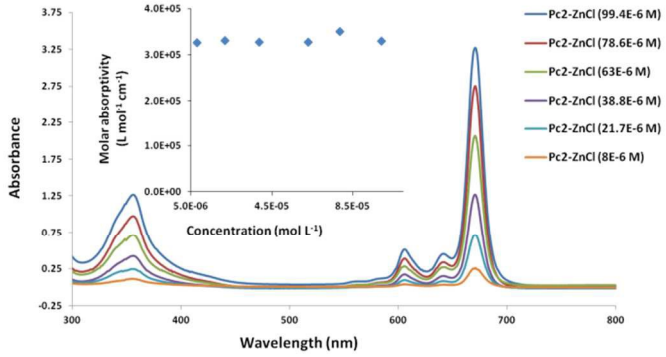

Fig. 3 UV-Vis spectra of **Pc2-Zn** in DMF at different concentrations ranging from 10 to 100 μM measured in cuvette with 1 mm path length, inset: dependence of the extinction coefficient at λ_{max} on the concentration of **Pc2-Zn**.

The UV-vis analysis was extended to evaluate the effect of halogen atoms by comparing the spectra of the prepared complexes with the previously reported non-halogenated **Pc1-Zn.** The Q-band of the **Pc2-Zn** containing 16 chlorine atoms is slightly blue-shifted in comparison to **Pc1-Zn (**ca 4 nm**)** due to the inductive effect exerted by the chlorine atoms which reduce the contribution of oxygen lone pairs of the aryloxy substituents to Pc core and consequently increase the HUMO-LUMO energy gap. This is supported by the slight red shifted Q-band position of **Pc3-Zn** (containing 16 bromine atoms) relative to that of **Pc2-Zn** which could be explained by the virtue of higher electronegativity of chlorine over that of bromine atoms.

The absorption spectra of the prepared complexes containing different metals were also examined to confirm the impact of size and electronic effect of the inserted metals. We found that the insertion of different transition metals within the Pc cores can tune their Q-band position due to the destabilization of the Pc π-system. As shown in (Table 3), the indium central metal produced the largest red shift followed by the gallium metal ion as compared to the corresponding zinc derivatives. This can be attributed either to the distortion of D_{4h} symmetry due to the displacement of indium out of the π-plane structure creating non-planar system or to the weakness of the coordination bond arising from the decreased electronegativity of the inserted metal.

Single crystal X-ray diffraction analysis

Crystal structure of Pc2-Zn. The molecular structure of **Pc2-Zn** obtained from single crystal X- ray diffraction data is given in Fig. 4. Similar to its phthalonitrile precursor, the aromatic planes of the phenoxy substituents containing chlorine atoms are oriented perpendicular to the plane of the phthalocyanine core. This arrangement makes half of the chlorine atoms directed upward with respect to the phthalocyanine plane and the other half is directed downward Fig. 4B. As pointed out earlier, such orthogonal orientation is the most effective strategy to avoid cofacial self-association of Pcs, thereby enabling them to remain truly nonaggregated in dissolved conditions. It was also observed that in its crystal packing (see Supporting information), the fifth position of the zinc atom in the phthalocyanine is coordinated to an axial pyridine molecule (few drops of pyridine were added to the concentrated solution of the complex to help in growing good crystal quality by simple diffusion method). The packing of **Pc2-Zn** molecules within the crystal network is observed to be very efficient utilizing variety of possible nonbonding interactions. The chlorine atoms in neighboring structures are oriented as far as possible to avoid steric hindrance. The minimum Cl-Cl distance detected is 3.54 Å, well above the normal Cl-Cl bond length (1.99 Å) and greater than sum of its Van der Waals radii. The available free space resulting from this arrangement is occupied by THF molecule which provides extra stability by non-bonding interactions to prevent deterioration of the crystal network. More discussion on the crystal structure and the packing pattern of **Pc2-Zn** is given in supporting information.

The structural features of phthalocyanine precursors and **Pc2-Zn** obtained from X-ray diffraction analysis can be considered to be similar under solution conditions as well. Therefore, the monomeric nature of the various Pc-M systems confirmed by NMR and UV-Vis spectral analysis can be attributed to the steric constraints imposed by the bulky halogen-containing phenoxy substituents as discussed before.

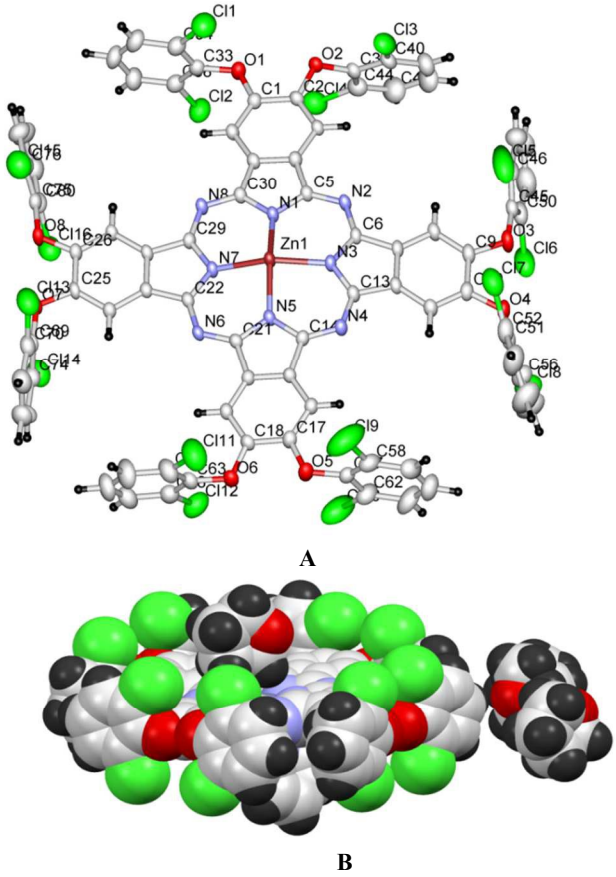

Fig. 4 Crystal structure of **Pc2-Zn**; (A) Thermal ellipsoid representation, (B) Space filling illustration showing the perpendicular orientation of chlorine atoms with respect to the Pc core and the occupancy of one of the THF solvent within the molecular cage. A molecule of pyridine is coordinated from below (A few drops of pyridine were added to develop good crystal). Color code: red - oxygen; blue - nitrogen; gray - carbon; green - chlorine; black - hydrogen.

Theoretical calculations

All geometry optimizations were performed using D_{4h} symmetry [50] in gas phase. The most important bond distances and angles listed in Table S6, and the labeling scheme is presented in Fig. 5. The optimized structure of **Pc2-Zn** (Fig. 5 and Table S4) is in good agreement with the crystal structure determined by X-ray analysis Fig. 4, which confirms the perpendicular orientation of phenoxy groups in respect to Pc core of the studied complexes (**Pc1-Zn**, **Pc2-Zn** and **Pc3-Zn**). In general, the unsubstituted ZnPc is reported to have perfectly planar structure. [51] However, it was noted that the halogen atoms directly attached to porphyrin core at both α and β positions caused a structural deformation.[52] This deformation led to significant changes in the energy levels and consequently the position of the Q and B-bands.[52] Our results showed that the halogenated phenoxy groups on Pc have a smaller distortion effect than the halogens directly attached to porphyrin core.[52] The out of plane deformations are negligibly small and therefore, all complexes retained D_{4h} symmetry. Accordingly, their UV-visible spectra were not affected.

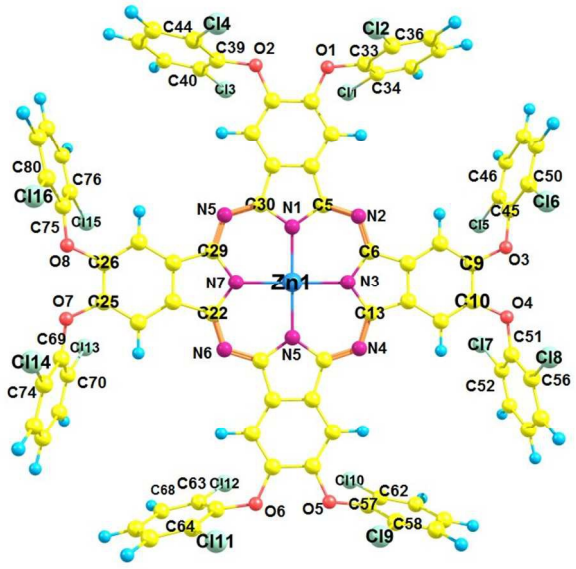

Fig. 5 Optimized structure of **Pc2-Zn** using B3LYP/SDD showing the perpendicular orientation of chlorine atoms with respect to Pc core. Color code: red - oxygen; magenta - nitrogen; yellow - carbon; green - chlorine; blue – hydrogen; dark blue - zinc.

The electronic structure and vertical excitation energy were calculated to gain further insight into the optical and electronic properties for **Pc2-Zn** and **Pc3-Zn** along with **Pc1-Zn** using DFT approach, which can deduce accurate structures and spectroscopic properties of organometallic porphyrins and phthalocyanines.[26-33] Such calculations can rationalize the observed spectral features based on the molecular structures of the studied complexes. Time-dependent density functional theory (TD-DFT) calculations for **Pc1-Zn**, **Pc2-Zn** and **Pc3-Zn** were performed to study the influence of the substituents on the electronic spectra, based on the geometries optimized at the B3LYP/SDD level. The results of TD-DFT calculations on selected electronic transitions with the corresponding oscillator strengths and excitation configurations of the target complexes are listed in Table 1. The molecular orbital energy diagrams calculated by a DFT approach are shown in Fig. 6, and the molecular orbital surfaces are depicted in Fig. 7 and Fig. S12.

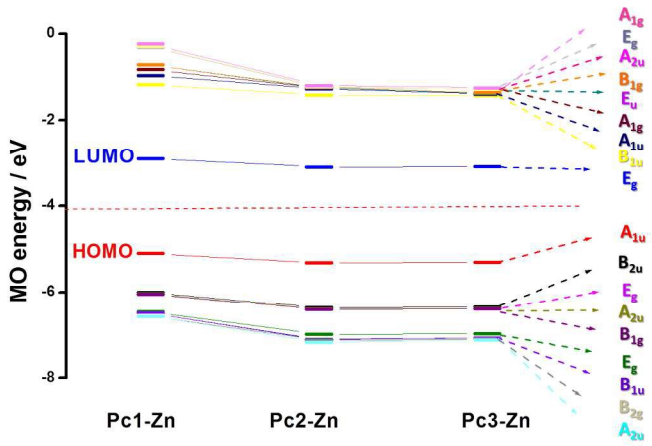

Fig. 6 Molecular energy level predicted for (**Pc1-Zn**, **Pc2-Zn** and **Pc3-Zn**).

Table 1. Calculated major excitation energies (ΔE in eV) and oscillator strengths (*f*) for **Pc1-Zn**, **Pc2-Zn** and **Pc3-Zn** obtained at the B3LYP/SDD level.

Compound	ΔE/eV	*f*	Main configuration	λ_{max} (nm)	coefficient	assignment
Pc1-Zn	2.0027	0.4783	H→L+1	619	0.67173	π-π*
	2.7754	0.3707	H-4→ L	446	0.62514	π-π*
	2.7817	0.4405	H-4→L+1	445	0.47044	π-π*
	3.3330	0.0231	H-8→L	371	0.39858	π-π*
Pc2-Zn	2.0474	0.4371	H→L	605	0.68022	π-π*
	2.0480	0.4364	H→L+1	606	0.68013	π-π*
	2.9401	0.4375	H-4→L	421	0.66382	π-π*
	2.9409	0.4368	H-4→L+1	421	0.66441	π-π*
	3.5939	0.4397	H-10→L	344	0.66161	π-π*
	3.5948	0.4414	H-10→L+1	344	0.66032	π-π*
Pc3-Zn	2.0428	0.4413	H→L	606	0.67219	π-π*
	2.0429	0.4411	H→L+1	606	0.67217	π-π*
	2.9332	0.4351	H-4→ L	422	0.53639	π-π*
	2.9333	0.4353	H-4→L+1	422	0.53664	π-π*
	3.5699	0.3765	H-8→L	347	0.55731	π-π*
	3.5701	0.3759	H-8→L	347	0.55593	π-π*

The UV/Vis absorption spectrum is based mainly on the vertical transition between molecular energy levels, which determine the position of the B and Q bands. Thus, we investigated the molecular energy levels and the vertical transition energy to explore the halogenation effects on photophysical properties. From Table 1, the absorption spectra of the non-halogenated **Pc1-Zn** consists of four main transitions. The first electron transition related to the Q-band (HOMO→LUMO+1) observed at (λ_{max} = 619 nm), which corresponds to the experimentally obtained band at 675 nm in the UV-vis spectra shown in Fig. 8. The B-band spectra consists of 3 main transitions observed at 446, 445 and 371 nm. The calculated band around 371 nm corresponded to the experimentally measured peak at 359 nm shown in Fig. 8. The halogenated complexes **Pc2-Zn** (λ_{max} = 605 nm) and **Pc3-Zn** (λ_{max} = 606 nm) exhibited ca 14 nm hypsochromic shift of the Q-band as compared to **Pc1-Zn** (619 nm) at the same level of theory (Fig. 8). Both **Pc2-Zn** and **Pc3-Zn** complexes were composed of six main transitions. The Q-band region consists of two transitions (HOMO→LUMO, LUMO+1) observed at ca 606 nm. The other transitions observed at 421 and 334 nm corresponded to B-band (Table 1). Moreover other weak transitions appeared at 466 and 396 nm and were attributed to n→π* transitions in case of **Pc1-Zn**. Such weak transitions were observed as a small shoulder around (430 nm) in the experimentally determined UV-vis spectra (Fig. 8~~A~~) and calculated at (421 nm) as shown in Fig. 8~~B~~ and depicted in Table 1. This shoulder were arises from n→π* transitions of lone pair of electrons of the ether oxygen.[53] The band around 421 nm were reported as a Ligand- Metal charge transfer (LMCT) absorption band shown in Fig. 7 and Fig S12.[54] These n→π* transitions were also observed for both **Pc2-Zn** and **Pc3-Zn** as Ligand to Metal charge transfer (LMCT) shown in Fig. 7 and Fig S12. The MLCT and LMCT can be represented by b_{1g}, b_{2g}, e_u, a_{1g} and e_u molecular orbitals as shown in Fig. 7 and Fig S12. The HOMO is represented by a a_{1u} π-orbital, while the LUMO consists of degenerate e_g π-orbitals, as supposed by the classic Gouterman's four-orbital orbital scheme description.[55] The DFT calculations show a significant stabilization of the a_{2u} (HOMO-4) π-orbital in comparison to the b_{2u} (HOMO-1) in the studied complexes. However, in case of both halogenated complexes (**Pc2-Zn** and **Pc3-Zn**) a significant stabilization on the b_{1g} (HOMO-5) and b_{2g} (HOMO-6) (i.e. nitrogen lone-pair-based n-orbitals) occurs. Therefore, the metal-centred $d_{x^2-y^2}$ orbital for **Pc2-Zn** and **Pc3-Zn** has a significantly more contribution in the pyrrolic nitrogen-centred nonbonding b_{1g} molecular orbital than in the non-halogenated **Pc1-Zn**. Moreover, the LUMO+3 of the halogenated complexes (**Pc2-Zn** and **Pc3-Zn**) is mainly localized over the phenoxy groups shown in Fig.8 and Fig S12.

Journal Name RSCPublishing

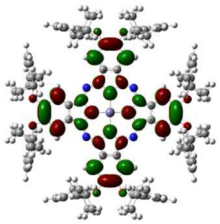	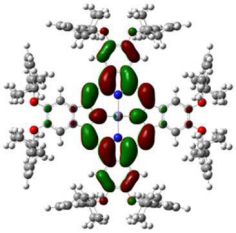	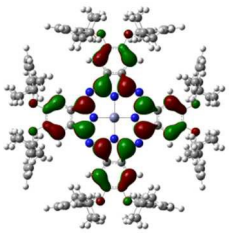	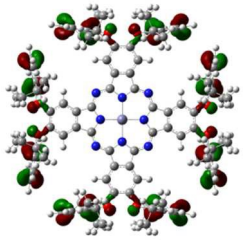	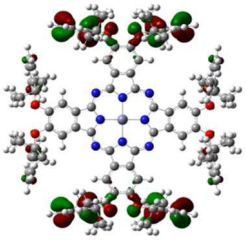
(LUMO+3, b_{2u})	(LUMOs, e_g)	(HOMO, a_{1u})	(HOMO-5, a_{2g})	(HOMO-6, e_u)
Pc1-Zn				
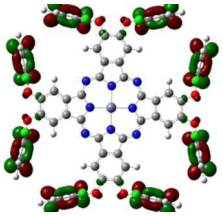	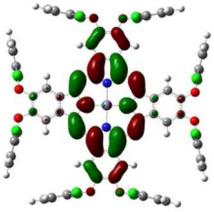	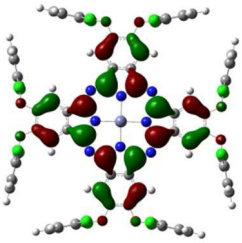	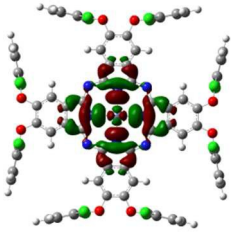	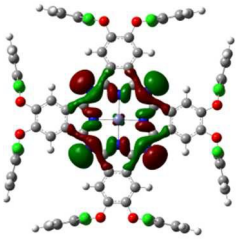
(LUMO+3, a_{1g})	(LUMOs, e_g)	(HOMO, a_{1u})	(HOMO-5, b_{1g})	(HOMO-6, b_{2g})
Pc2-Zn				
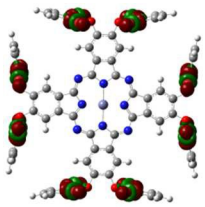	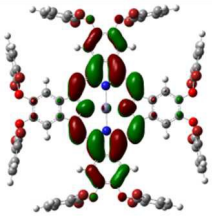	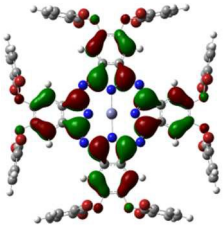	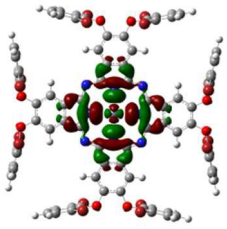	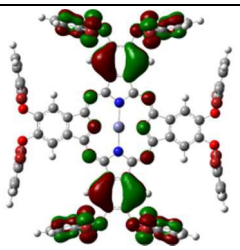
(LUMO+3, a_{1g})	(LUMOs, e_g)	(HOMO, a_{1u})	(HOMO-5, b_{1g})	(HOMO-6, e_g)
Pc3-Zn				

Fig. 7 Molecular orbital surfaces of some selected HOMOs and LUMOs for **Pc1-Zn**, **Pc2-Zn** and **Pc3-Zn**.

Table 2. Energies of HOMO and LUMO levels, and energy gap (ΔE) at B3LYP/SDD, in eV.

	HOMO	HOMO-1	HOMO-2	HOMO-3	HOMO-4	LUMO	LUMO+1	LUMO+2	LUMO+3	LUMO+4	ΔE(eV) LUMO-HOMO
Pc1-Zn	-5.01	-6.00	-6.04	-6.04	-6.04	-2.88	-2.87	-1.14	-0.970	-0.821	2.19
Pc2-Zn	-5.315	-6.361	-6.396	-6.396	-6.414	-3.098	-3.098	-1.413	-1.272	-1.246	2.22
Pc3-Zn	-5.309	-6.352	-6.387	-6.387	-6.405	-3.095	-3.095	-1.427	-1.393	-1.376	2.21

Journal Name RSCPublishing

Table 3. Photophysical properties of studied complexes in THF.[a]

Complex	λ_{max} (nm)	λ_{em} (nm)	ε_{max} (M^{-1} cm^{-1})	Φ_F[b, c]	Φ_Δ[b, d]
Pc2-Mg	672	676	2.96×10^5	0.62	0.21
Pc2-Zn	671	675	3.35×10^5	0.33	0.53
Pc2-Ga	683	688	2.49×10^5	0.23	0.52
Pc2-In	691	695	2.40×10^5	0.030	0.83
Pc3-Mg	675	679	2.76×10^5	0.50	0.24
Pc3-Zn	673	676	3.27×10^5	0.32	0.53
Pc3-Ga	684	692	2.96×10^5	0.19	0.56
Pc3-In	693	698	3.01×10^5	0.028	0.82

[a] absorption maximum at the Q-band (λ_{max}), emission maximum (λ_{em}), extinction coefficient (ε_{max}), fluorescence quantum yield (Φ_F) and singlet oxygen quantum yield (Φ_Δ). [b]mean of three independent measurements, estimated error: ±10%; [c] with ZnPc as reference (Φ_F in THF = 0.32); [d] with ZnPc as reference (Φ_Δ in THF = 0.53)

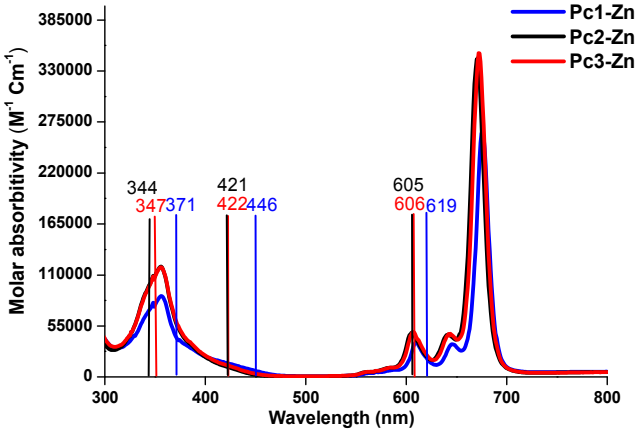

Fig. 8 :Comparison between gas phase (bars) and the experimentally observed UV-Vis spectra of **Pc1-Zn**, **Pc2-Zn** and **Pc3-Zn.**

Photophysics

Fluorescence emission spectra were collected in THF. They had a typical shape for this type of complexes and they mirrored the absorption spectra in the Q-band area (Fig. 9 and Fig. S14). The excitation spectra perfectly overlapped the absorption spectra Fig. S14 that further confirmed that the complexes were present exclusively in monomeric form and that the aggregates did not influence determination of photophysical parameters.

Fluorescence quantum yields (Φ_F) were determined in THF with ZnPc as the reference (Φ_F in THF = 0.32). The values of Φ_F were substantially influenced by presence of the central metal (Table 3). The strongest fluorescence was obtained for Mg derivatives followed by GaCl and Zn complexes. Fluorescence of InCl complexes was always very weak. Reversely to the central cation, effect of peripheral halogen can be considered as negligible (if any) and the observed difference between **Pc2-M** and **Pc-3M** series for the same central metal was within the experimental error.

Singlet oxygen quantum yields (Φ_Δ) were determined in THF by method of chemical trap (1,3-diphenylisobenzofuran) with ZnPc as reference (Φ_Δ in THF = 0.53). The order of the Φ_Δ values for complexes with different central metal was reversed to one observed for fluorescence (Table 3), i.e. InCl > GaCl ~ Zn > Mg. Similarly to fluorescence, the differences between chlorinated (**Pc2-M**) and brominated (**Pc3-M**) series felt within the experimental error.

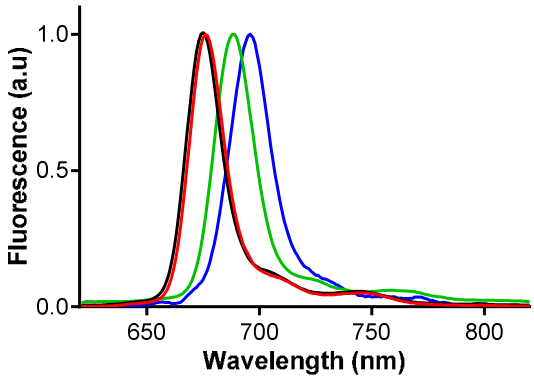

Fig. 9 Emission spectra of **Pc2-Mg** (red), **Pc2-Zn** (black), **Pc2-Ga** (green) and **Pc2-In** (blue) in THF, λ_{exc} = 610 nm.

The results from photophysical measurements can be easily interpreted as heavy atom effect of the central cation. The heavy atom effect, described for the first time by McClure,[56] shifts the probability of the singlet excited state relaxation toward intersystem crossing (here represented by Φ_Δ values) on the account of photon emission. The influence of the metal cation in the current series was very strong as can be easily seen from steep dependences of the

quantum yields on atomic weight of the central metal Fig. 10. On the other hand, the effect of halogen substituents was very weak. This fact was further confirmed by comparison of the photophysical data of **Pc2-Zn** and **Pc-3Zn** with unsubstituted ZnPc that was used as reference. Both phenoxy substituted zinc complexes reached the same Φ_F and Φ_Δ values as the reference compound (Table 3). This fact indicates that not only the halogen but actually the whole halogenated phenoxy substituent did not affect the photophysics at all and the changes were induced by central metal only.

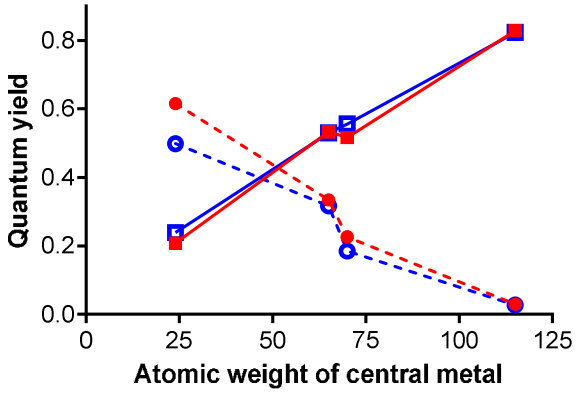

Fig. 10 Φ_F (circles, dashed lines) and Φ_Δ (squares, full lines) values of chlorinated **Pc2-M** (red, full symbols) and brominated **Pc3-M** (blue, open symbols) in THF in dependence on the atomic weight of the central metal.

Conclusions

Eight new Pc derivatives with halogenated phenoxy peripheral substituents were synthesized and characterized. Presence of bulky halogens in *ortho* positions on phenoxy substituents forced them to keep perpendicular orientation towards the Pc plane as predicted by theoretical calculations and unequivocally confirmed by single crystal X-ray diffraction. NMR and UV-vis studies confirmed that such spatial arrangement inhibits fully aggregation in organic solvents and keeps the molecules of Pc separated in solution as monomers even at high concentrations. DFT calculations were used to discuss the differences in absorption spectra of halogenated and non-halogenated Pcs. Strong influence of the central metal on photophysical properties (Φ_F and Φ_Δ values) was observed and attributed to heavy atom effect. .

Acknowledgements

The authors acknowledge the support of this work by the Research Administration of Kuwait University, under the Grant Number SC01/09, the facilities of GFS (GS01/01, GS03/01.GS03/08).

Notes and references

[a] Department of Chemistry, Kuwait University, P.O. Box 5969, Safat 13060, Kuwait.
[b] Department of Biophysics and Physical Chemistry, Faculty of Pharmacy in Hradec Kralove, Charles University in Prague, Heyrovskeho 1203, Hradec Kralove 50005, Czech Republic.
[c] Department of Pharmaceutical Chemistry and Drug Control, Faculty of Pharmacy in Hradec Kralove, Charles University in Prague, Heyrovskeho 1203, Hradec Kralove 50005, Czech Republic.

† Footnotes should appear here. These might include comments relevant to but not central to the matter under discussion, limited experimental and spectral data, and crystallographic data.

Electronic Supplementary Information (ESI) available: [details of any supplementary information available should be included here]. See DOI: 10.1039/b000000x/

1 N. B. McKeown, *Phthalocyanine materials: synthesis, structure and function*; Cambridge University Press: Cambridge, 1998.
2 P. Gregory, *J. Porphyrins Phthalocyanines*, 2000, **4**, 432-437.
3 C. G. Claessens, U. Hahn and T. Torres, *Chem. Rec.*, 2008, **8**, 75-97.
4 C.C. Leznoff, A. B. P. Lever, *Phthalocyanines, Properties and Applications*; VCH: NewYork, 1989; Vol. 1-4.
5 V. N. Nemykin, E. A. Lukyanets, *Arkivoc* 2010, 136.
6 G. de la Torre, P. Vázquez, F. Agulló-López and T. Torres, *Chem. Rev.*, 2004, **104**, 3723-3750.
7 D. Dini, M. Hanack and M. Meneghetti, *J. Phys. Chem. B*, 2005, **109**, 12691-12696.
8 S. Vagin, M. Barthel, D. Dini and M. Hanack, *Inorg. Chem.*, 2003, **42**, 2683-2694.
9 P. Zimcik, M. Miletin, J. Ponec, M. Kostka and Z. Fiedler, *J. Photochem. Photobiol., A*, 2003, **155**, 127-131.
10 V. Novakova, R. Z. U. Kobak, R. Kučera, K. Kopecky, M. Miletin, V. Krepsová, J. Ivincová and P. Zimcik, *Dalton Trans.*, 2012, **41**, 10596-10604.
11 S. Makhseed, M. Machacek, W. Alfadly, A. Tuhl, M. Vinodh, T. Simunek, V. Novakova, P. Kubat, E. Rudolf and P. Zimcik, *Chem. Commun.*, 2013, **49**, 11149-11151.
12 P. Zimcik, V. Novakova, K. Kopecky, M. Miletin, R. Z. U. Kobak, E. Svandrlikova, L. Váchová and K. Lang, *Inorg. Chem.*, 2012, **51**, 4215-4223.
13 M. Machacek, A. Cidlina, V. Novakova, J. Svec, E. Rudolf, M. Miletin, R. Kučera, T. Simunek, and P. Zimcik, *J. Med. Chem.*, 2015, **58**, 1736-1749.
14 M. Brewis, G. J. Clarkson, P. Humberstone, S. Makhseed and N. B. McKeown, *Chem.-Eur. J.*, 1998, **4**, 1633-1640.
15 M. Brewis, B. M. Hassan, H. Li, S. Makhseed, N. B. McKeown and N. Thompson, *J. Porphyrins Phthalocyanines*, 2000, **4**, 460-464.
16 S. Makhseed, M. Al-Sawah, J. Samuel and H. Manaa, *Tetrahedron Lett.*, 2009, **50**, 165-168.
17 H. Manaa, A. A. Mulla, S. Makhseed, M. Al-Sawah and J. Samuel, *Opt. Mater.*, 2009, **32**, 108-114.
18 X.-J. Jiang, S.-L. Yeung, P.-C. Lo, W.-P. Fong and D. K. P. Ng, *J. Med. Chem.*, 2010, **54**, 320-330.
19 J. T. F. Lau, P.-C. Lo, Y.-M. Tsang, W.-P. Fong and D. K. P. Ng, *Chem. Commun.*, 2011, **47**, 9657-9659.
20 V. Mantareva, V. Kussovski, I. Angelov, D. Wöhrle, R. Dimitrov, E. Popova and S. Dimitrov, *Photochem. Photobiol. Sci.*, 2011, **10**, 91-102.
21 F. C. Rossetti, L. B. Lopes, A. R. H. Carollo, J. A. Thomazini, A. C. Tedesco and M. V. Bentley, *J. Control. Release*, 2011, **155**, 400-408.
22 S. Makhseed, J. Samuel, *Dyes Pigm.*, 2009, **82**, 1-5.
23 N. B. McKeown, S. Makhseed, K. J. Msayib, L. L. Ooi, M. Helliwell and J. E. Warren, *Angew. Chem., Int. Ed.*, 2005, **44**, 7546-7549.
24 T. Nyokong, *Coord. Chem. Rev.*, 2007, **251**, 1707-1722.
25 A. Tuhl, H. Manaa, S. Makseed, N. Al-Awadi, J. Mathew, H. M. Ibrahim, *Opt. Mater.*, 2012, **34**, 1869-1877.
26 X.-F. Zhang and H.-J. Xu, *J. Chem. Soc. Faraday Trans.*, 1993, **89**, 3347-3351.

27 J. E. Van Lier, C. M. Allen and W. M. Sharman, *J. Porphyrins Phthalocyanines*, 2001, **5**, 161-169.
28 E. A. Lukyanets, V. N. Nemykin, *J. Porphyrins Phthalocyanines*, 2010, **14**, 1-40.
29 E. A. Makarova, E. A. Lukyanets, *J. Porphyrins Phthalocyanines*, 2009, **13**, 188-202.
30 S. P. Keizer, J. Mack, B. A. Bench, S. M. Gorun and M. J. Stillman, *J. Am. Chem. Soc.*, 2003, **125**, 7067–7085.
31 V. N. Nemykin, R. G. Hadt, R. V. Belosludov, H. Mizuseki, Y. Kawazoe, *J. Phys. Chem. A*, 2007, **111**, 12901-12913.
32 G. Ricciardi, A. Rosa and E. J. Baerends, *J. Phys. Chem. A*, 2001, **105**, 5242-5254.
33 Y. Zhang, X. Zhang, Z. Liu, Y. Bian and J. Jiang, *J. Phys. Chem. A*, 2005, **109**, 6363-6370.
34 L. Yang, L. Guo, Q. Chen, H. Sun, J. Liu, X. Zhang, X. Pan and S. Dai, *J. Mol. Graphics Modell.* 2012, **34**, 1-9.
35 D. Wöhrle, M. Eskes, K. Shigehara and A. Yamada, *Synthesis*, 1993, 194-196.
36 D.D. Perrin, W.L.F. Armarego: *Purification of laboratory chemicals*; 3rd ed.; Pergamon Press: Oxford, **1988**.
37 M. Dolg and H. Stoll, *Theor. Chim. Acta*, 1993, **85**, 441-450.
38 A. Bergner, M. Dolg, W. Kuechle and H. Stoll, *Mol. Phys.* 1993, **80**, 1431-1441.
39 M. J. Frisch, G. W. Trucks, H. B. Schlegel, G. E. Scuseria, M. A. Robb, J. R. Cheeseman, G. Scalmani, V. Barone, B. Mennucci, G. A. Petersson, H. Nakatsuji, M. Caricato, X. Li, H. P. Hratchian, A. F. Izmaylov, J. Bloino, G. Zheng, J. L. Sonnenberg, M. Hada, M. Ehara, K. Toyota, R. Fukuda, J. Hasegawa, M. Ishida, T. Nakajima, Y. Honda, O. Kitao, H. Nakai, T. Vreven, Jr. J. A. Montgomery, J. E. Peralta, F. Ogliaro, M. Bearpark, J. J. Heyd, E. Brothers, K. N. Kudin, V. N. Staroverov, R. Kobayashi, J. Normand, K. Raghavachari, A. Rendell, J. C. Burant, S. S. Iyengar, J. Tomasi, M. Cossi, N. Rega, N. J. Millam, M. Klene, J. E. Knox, J. B. Cross, V. Bakken, C. Adamo, J. Jaramillo, R, Gomperts, R. E. Stratmann, O. Yazyev, A, J. Austin, R. Cammi, C. Pomelli, J. W. Ochterski, R. L. Martin, K. Morokuma, V. G. Zakrzewski, G. A. Voth, P. Salvador, J. J. Dannenberg, S. Dapprich, A. D. Daniels, Ö. Farkas, J. B. Foresman, J. V. Ortiz, J. Cioslowski and D. J. Fox, Gaussian 09, Revision B.01, Gaussian, Inc.: Wallingford, CT, USA, 2010.
40 R. Dennington, T. Keith, J. Millam, GaussView, version 5, Semichem. Inc.: Shawnee Mission, KS, 2009.
41 Data Visualization Tools: ChemCraft, http://www.chemcraftprog.com. Accessed January, **24**, 2014.
42 V. Novakova, M. Miletin, T. Filandrová, J. Lenčo, A. Růžička and P. Zimcik, *J. Org. Chem.* 2014, **79**, 2082-2093.
43 L. Kaestner, M. Cesson, K. Kassab, T. Christensen, P. D. Edminson, M. J. Cook, I. Chambrier and G. Jori, *Photochem. Photobiol. Sci.* 2003, **2**, 660-667.
44 S. E. Maree, T. Nyokong, *J. Porphyrins Phthalocyanines*, 2001, **5**, 782-792.
45 S. Vagin, A. Frickenschmidt, B. Kammerer and M. Hanack, European *J. Organic Chemistry*, 2005, **2005**, 3271-3278.
46 E. N. Ovchenkova and T. N. Lomova, *Russ J Org Chem*, 2011, **47**, 1581-1587.
47 C.-F. Choi, P.-T. Tsang, J.-D. Huang, E. Y. M. Chan, W.-H. Ko, W.-P. Fong and D. K. P. Ng, *Chemical Communications*, 2004, 2236-2237.
48 W. Liu, T. J. Jensen, F. R. Fronczek, R. P. Hammer, K. M. Smith and M. G. H. Vicente, *J. Medicinal Chemistry*, 2005, **48**, 1033-1041.
49 M. Yoshioka, K. Ohta and M. Yasutake, *RSC Advances*, 2015, **5**, 13828-13839.
50 S. U. Lee, J. C. Kim, H. Mizuseki, Y. Kawazoe, Chem. - Asian J., 2010, 5, 1341-1346.
51 W. R. Scheid, W. J. Dow, *J. Am. Chem. Soc.*, 1977, **99**, 1101-1104.
52 H. Shahroosvand, S. Zakavi, A. Sousaraei, M. Eskandari, *Phys. Chem. Chem. Phys.*, 2015, **17**, 6347-6358.
53 Z. Musil, P. Zimcik, M. Miletin, K. Kopecky, P. Petrik, Juraj Lenco, *J. of Photochemistry & Photobiology, A: Chemistry*., 2007, **186**, 316-322.
54 Y. Zhang, X. Cai, X. Zhang, H. Xu, Z. Liu, J. Jiang, International Journal of Quantum Chemistry 2007, **107**, 952-961.
55 M. Gouterman, *J. Mol. Spectrosc*. 1961, **6**, 138-163.
56 D. S. McClure, *J. Chem. Phys.* 1949, **17**, 905-913.

